RAD51 Plays a Crucial Role in Halting Cell Death Program Induced by Ionizing Radiation in Bovine Oocytes 1

Authors: Kujjo, Loro L., Ronningen, Reg, Ross, Pablo, Pereira, Ricardo J.G, Rodriguez, Ramon, et al.

Source: Biology of Reproduction, 86(3) : 76

Published By: Society for the Study of Reproduction

URL: https://doi.org/10.1095/biolreprod.111.092064

BIOLOGY OF REPRODUCTION (2012) **86**(3):76, 1–11
Published online before print 21 December 2011.
DOI 10.1095/biolreprod.111.092064

RAD51 Plays a Crucial Role in Halting Cell Death Program Induced by Ionizing Radiation in Bovine Oocytes[1]

Loro L. Kujjo,[3,4,5] Reg Ronningen,[3,6] Pablo Ross,[7] Ricardo J.G. Pereira,[4] Ramon Rodriguez,[7] Zeki Beyhan,[7] Marcelo D. Goissis,[7] Thomas Baumann,[6] Wataru Kagawa,[8] Cagri Camsari,[7] George W. Smith,[7] Hitoshi Kurumizaka,[8] Shigeyuki Yokoyama,[9] Jose B. Cibelli,[4,7,10] and Gloria I. Perez[2,4,10]

[4]*Department of Physiology, Michigan State University, East Lansing, Michigan*
[5]*Department of Human Anatomy, Michigan State University, East Lansing, Michigan*
[6]*National Superconducting Cyclotron Laboratory (NSCL), Michigan State University, East Lansing, Michigan*
[7]*Department of Animal Sciences, Michigan State University, East Lansing, Michigan*
[8]*Laboratory of Structural Biology, Graduate School of Advanced Science and Engineering, Waseda University, Tokyo, Japan*
[9]*RIKEN Systems and Structural Biology Center, Yokohama, Japan*
[10]*LARCel, Programa Andaluz de Terapia Celular y Medicina Regenerativa, Sevilla, Spain*

ABSTRACT

Reproductive health of humans and animals exposed to daily irradiants from solar/cosmic particles remains largely understudied. We evaluated the sensitivities of bovine and mouse oocytes to bombardment by krypton-78 (1 Gy) or ultraviolet B (UV-B; 100 microjoules). Mouse oocytes responded to irradiation by undergoing massive activation of caspases, rapid loss of energy without cytochrome-*c* release, and subsequent necrotic death. In contrast, bovine oocytes became positive for annexin-V, exhibited cytochrome-*c* release, and displayed mild activation of caspases and downstream DNAses but with the absence of a complete cell death program; therefore, cytoplasmic fragmentation was never observed. However, massive cytoplasmic fragmentation and increased DNA damage were induced experimentally by both inhibiting RAD51 and increasing caspase 3 activity before irradiation. Microinjection of recombinant human RAD51 prior to irradiation markedly decreased both cytoplasmic fragmentation and DNA damage in both bovine and mouse oocytes. RAD51 response to damaged DNA occurred faster in bovine oocytes than in mouse oocytes. Therefore, we conclude that upon exposure to irradiation, bovine oocytes create a physiologically indeterminate state of partial cell death, attributed to rapid induction of DNA repair and low activation of caspases. The persistence of these damaged cells may represent an adaptive mechanism with potential implications for livestock productivity and long-term health risks associated with human activity in space.

apoptosis, *bovine*, *female germ cells*, *ionizing radiation*, *mouse*, *oocytes*, *RAD51*, *solar/cosmic radiation*

INTRODUCTION

Livestock kept in the open or grazing under the sun are subjected to not only pathophysiologic effects of heat stress but also to daily bombardment by irradiants of solar/cosmic origin (ultraviolet radiation, protons, neutrons, and nuclei of heavy elements and their decay products). Unfortunately, global warming and ozone depletion have contributed to the increase in magnitude of solar/cosmic radiation or of their decay products reaching the earth. It is estimated that approximately 75% of extraterrestrial direct normal irradiance passes through the atmosphere without being scattered or absorbed [1–7]; so, even at ground level, cosmic radiation is part of our normal environment.

Cosmic rays (CRs) are high-energy charged particles that originate in outer space mainly from supernova explosions but also from other stars. They travel at the speed of light, striking the earth at the rate of approximately 1 cosmic ray every cm^2 every minute from all directions, and their presence can still be detected even more than 1 mile below the earth's surface [8]. On average, CRs have a penetration depth in air of approximately 10 km; for comparison, x-rays are 100 times weaker, with an average penetration depth of 100 m. During a regular night's sleep, an average of 1 million CRs will travel through a person's body [9].

Energetic CRs have damaging effects on living organisms, which are substantially greater than those of x-rays or gamma-rays [10, 11]. Because this high-frequency radiation has enough energy to remove electrons from atoms or molecules, their direct effects due to passage through the body can leave molecules momentarily ionized. Such ionized particles are unstable and quickly undergo chemical changes; and, as shown in studies by Nobel prize winner H.J. Muller [12] and others [13, 14], ionization can cause, among other effects, mutations and changes in human genes. There are also reports of DNA strand breaks [15, 16] and decreased capacity of the immune system [17]. Moreover, there is convincing evidence that irradiated cells can send out signals or release harmful substances that can result in the damage of nearby unirradiated cells, a phenomenon known as the bystander effect of radiation [18–21]. One wonders whether the direct or bystander effects of CRs are responsible for the reported association between CRs and death due to sudden cardiac arrest [22] or the incidence of the genetic damage(s) that triggers a significant fraction of human cancers in the general population (at ground level) [23] and in humans working at high altitudes (e.g., pilots

[1]Supported by the College of Veterinary Medicine, the Department of Physiology, the National Superconducting Laboratory (NSCL) at Michigan State University, and Fundacion Progreso y Salud (Seville, Spain).
[2]Correspondence: Gloria I. Perez, Michigan State University, Department of Physiology, 4173 BPS, East Lansing, Michigan 48824.
E-mail: perezg@msu.edu
[3]These authors contributed equally to this work.

Received: 28 February 2011.
First decision: 11 April 2011.
Accepted: 25 November 2011.

eISSN: 1529-7268 http://www.biolreprod.org
ISSN: 0006-3363

and other air crew members) [24, 25]. Of particular interest to us are the findings that fertility levels are lower among some high-altitude human populations [26]. Although low oxygen pressure was thought to be the main causative factor, it is equally possible to speculate that CRs were responsible for the observed subfertility in those populations, as a link between infant mortality rate and density of cosmic radiation has also been proposed [27]. More recently, it was observed that sperm at high altitude exhibit alterations of both the mitochondrial DNA copy number and the integrity of the nuclear DNA and, therefore, the possibility that male fertility is directly affected [28]. Interestingly, due to the effect of CRs on living organisms, these particles are also considered a possible cause of mass extinctions [29–31], and changes in their energetic activity have even been suggested to have a possible impact on the history of ancient civilizations [32].

We are not aware of similar studies in animal populations, except for few studies carried out in nonmammalian models (i.e., embryos from Japanese medaka, *Oryzias latipes* [33], and *Xenopus laevis* [34]), in which the biological damage associated with high-energy neutrons ranged from increased apoptosis in the developing brain to abnormal morphogenesis and death. The impact of CRs on the health of mammalian species, particularly livestock, remains largely undetermined. Hence, we were motivated to investigate these aspects of CR irradiation and specifically to determine their role as one of the causative factors of unexplained infertility in cattle.

Infertility is the diminished capacity or inability to produce viable and healthy offspring. In certain cases, the causative factors for infertility are relatively easy to determine; for example, aging, diseases, and disorders that directly affect female reproductive organs and related hormones are major causes of infertility [35–37]. In many other instances, however, when the causative factors cannot be identified, the inability to reproduce is referred to as ''unexplained'' or ''idiopathic'' infertility. Many studies have implicated unexplained infertility as one of the most important causes of culling and high economic loss in cattle farming [38].

We propose that one potential cause of unexplained infertility in cattle is the damage sustained by their germ cells as a consequence of daily irradiance from solar/cosmic particles. As discussed earlier, particles of cosmic origin have the capacity to penetrate tissues and traverse the whole body without losing all their energy [6, 39], and, as they traverse, they cause ionization and consequently DNA damage in various cell types, including germ cells in the ovaries.

We believe that continuous exposure of cattle to sublethal doses of ionizing radiation from solar/cosmic particles has evolutionarily induced oocytes to develop a rapid DNA repair mechanism, which is plagued with aberrant repairs. Oocytes bearing such repairs are fertilizable, but the ensuing embryos undergo fetal/perinatal mortality, thus affecting the overall fertility of cattle. The consequences of such events for the reproductive health of cattle have not been evaluated, yet they could be responsible for a percentage of the reported unexplained infertility problems (clinical or subclinical).

In the bovine family, fertility is highly compromised in cows receiving embryos that have sustained DNA damage from events such as handling during nuclear transfer [40]. Despite DNA damage, in vitro preimplantation embryo development is not affected at all. Nevertheless, the percentage of live born calves and their survival are extremely low. These observations coupled with the ability of charged energetic particles to induce ionization, led us to hypothesize that solar/cosmic particles penetrating body tissues are capable of inducing DNA double-strand breaks (DSBs) in oocytes and that bovine oocytes have evolved a quick repair mechanism to handle DNA damage from ionizing radiation. In mouse oocytes, we and others have recently demonstrated that RAD51, a protein involved in the homologous repair of DNA DSBs is a critical determinant of the cell's fate [41–43]. Because this protein is highly conserved among species, we also expect RAD51 to be of paramount importance for the survival and death of bovine oocytes. The present experiments were designed to evaluate the sensitivities of bovine and mouse oocytes to irradiation effects of solar/cosmic particles by using krypton (Kr-78) or ultraviolet-B (UV-B) radiation as an example. It should be noted here that the primary CRs hitting the earth's atmosphere consist of a flux of particles originating from galactic sources and solar winds. These particles are made up of 92% protons, 6% alpha particles, and 2% heavier atomic nuclei [44]. Collision of the primary rays with atmospheric atoms triggers a cascade of secondary particles, with consequential final energy levels hitting the terrestrial surfaces constituting fewer than 1% of the original primary flux. High-energy high-Z isotopes such as Kr-78 (mass number [A] = 78; atomic number [Z] = 36) used in our experiments may constitute negligible amounts in the secondary cosmic flux and would be broken up upon collision with atmospheric atoms. Hence, Kr-78 was used in our experiments to simulate a dose of energy from primary CRs or cascade particles that would be incident at sea level.

MATERIALS AND METHODS

Bovine Oocyte Collection and Maturation

Cows' ovaries were collected from a local abattoir and transported to the laboratory in warmed PBS containing antibiotics. Cumulus-oocyte complexes (COC) were aspirated from follicles of 3–5 mm in size. COCs were matured for 24 h (at 39°C in a humidified atmosphere of 5% CO_2-95% air) in medium 199 supplemented with fetal bovine serum, follicle-stimulating hormone, luteinizing hormone, sodium pyruvate, and gentamicin sulfate. The next day, mature oocytes were denuded of cumulus cells with hyaluronidase and randomized into treatment groups in triplicates (100 metaphase II [MII] oocytes/tube, containing HEPES-buffered hamster embryo culture medium; [HH] medium). The tubes were taken to the National Superconducting Laboratories (NSCL) cyclotron for irradiation (Fig. 1).

Bovine In Vitro Fertilization

Mature oocytes were transferred into tyrode albumin lactate pyruvate-based fertilization medium [45]. Frozen-thawed sperm was selected by Percoll (Sigma-Aldrich) gradient and added to the medium containing the oocytes at 1×10^6 sperm cells/ml. Fertilization was carried out for 18 h at 38.5°C in 5% CO_2 in high humidity. Presumptive zygotes were cultured under mineral oil in simplex optimization medium with potassium and amino acids (KSOMaa; Millipore) supplemented with 3 mg/ml bovine serum albumin (BSA; Sigma).

Parthenogenetic Activation of Bovine Oocytes

Mature oocytes were denuded of cumulus cells with hyaluronidase (1 mg/ml) and vortexing. Denuded oocytes were activated using 5 μM ionomycin in HH medium for 4 min. Presumptive zygotes were placed in drops of 2 mM 6-dimethylaminopurine (DMAP; Sigma) in culture medium (KSOM) and incubated for 4 h at 38.5°C in 5% CO_2 and high humidity [46]. After this, parthenogenetic zygotes were placed in drops of KSOM and cultured as described for in vitro fertilization (IVF).

Mouse Oocyte Collection

The female mice used in all experiments were purchased from Charles River Laboratories. Mice were kept in well-controlled animal housing facilities and had free access to water and food. All experiments involving animals described herein were reviewed and approved by the institutional animal care and use committee of Michigan State University. Mice were superovulated with 10 IU of equine chorionic gonadotropin (Professional Compounding Centers of

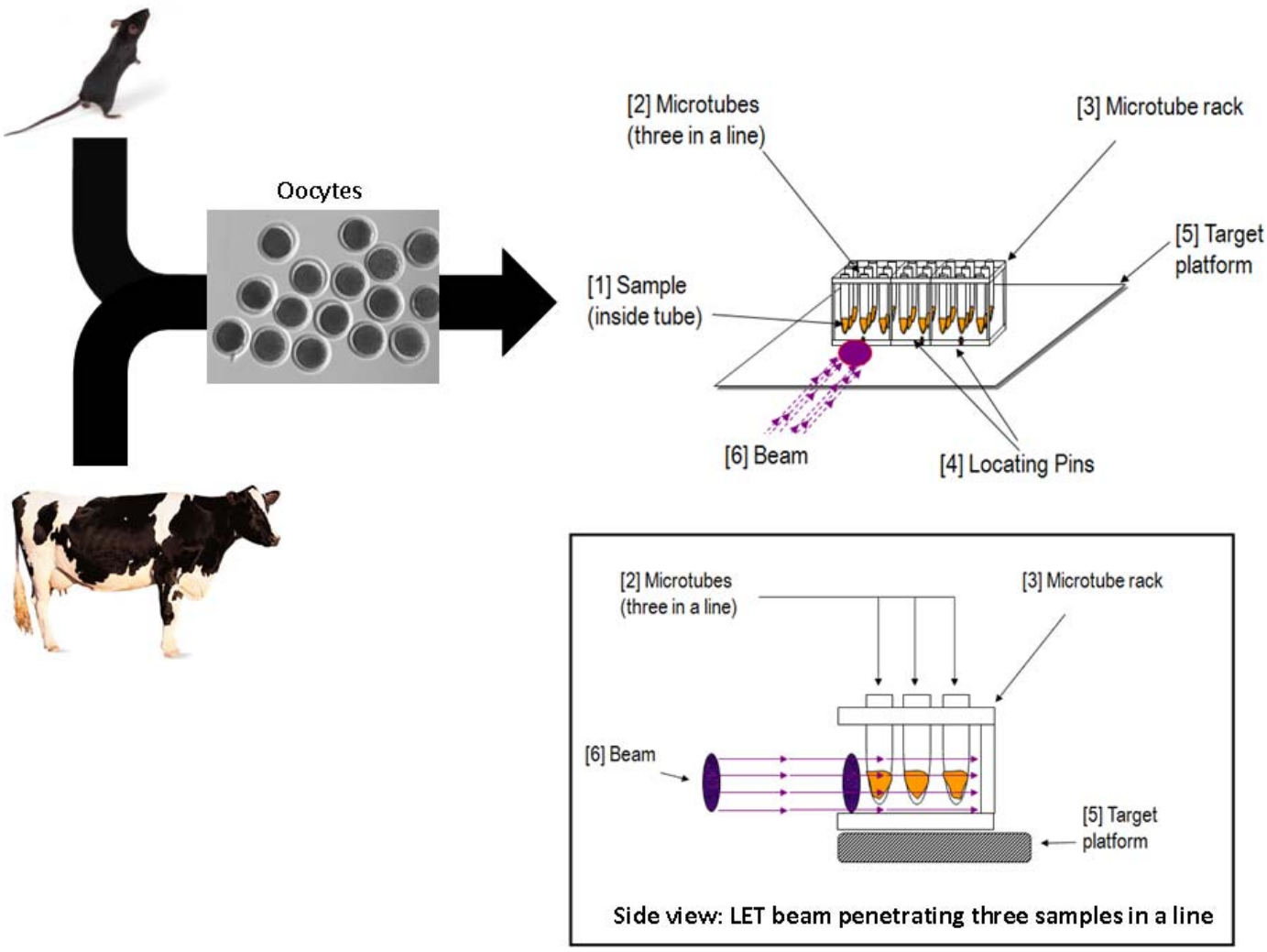

FIG. 1. Schematic representation of samples arranged for irradiation. Mature oocytes were collected from both mouse and bovine. After cumulus cells were removed, oocytes were transferred into 1.5-ml tubes and randomized to treatment groups in triplicates. All tubes were arranged on a microtube rack designed for the experiments. This rack contains slots in 8 lanes labeled A–H and 5 rows labeled 1–5, spaced to ensure that the beam strikes only 1 sample per lane and penetrates all 3 samples in a row without significant loss in energy. The rack was set on top of the target platform inside the irradiation room, and irradiation of samples was accomplished via a remote computerized system fitted with video cameras and located outside the irradiation room. By focusing on the locating pins on the rack via the camera, the beam could be positioned accurately. Following irradiation, the specimens were transported back to the laboratory.

America, Houston, TX), followed by 10 IU of human chorionic gonadotropin (hCG; Serono Laboratories, Norwell, MA) 46 h later. Mature oocytes were collected from the oviducts 16 h after hCG injection. COCs were denuded of cumulus cells by a 1-min incubation in a solution of 80 IU/ml hyaluronidase (Sigma, St. Louis, MO), followed by 3 washes with culture medium. Mature oocytes were then randomized to treatment groups in triplicates (100 MII oocytes/tube) and taken to the NSCL cyclotron for irradiation (Fig. 1).

Irradiation

Linear energy transfer (LET) irradiation of all samples was performed at the NSCL on the MSU campus. Before and during irradiation, samples were maintained in HH medium at room temperature. Samples assigned to treatment groups were irradiated (Fig. 1) for various times (30–420 sec) with Kr-78 ions at 150 MeV/nucleon (an approximate kinetic energy of 11.7 GeV) [6]. Each group received 1 Gy of LET radiation. Controls included (a) one group of unirradiated oocytes and (a) one group that was subjected to all manipulations except irradiation. Following irradiation, the specimens were transported back to the laboratory, and half were immediately analyzed for DNA damage. The remaining samples were transferred into fresh culture medium and incubated for various periods of time. In some experiments, oocytes were exposed to UV-B irradiation (100 microjoules) before incubation.

Oocyte Culture

Immediately after irradiation, all bovine and mouse oocytes were transported to our laboratory and incubated for 6–24 h at 39°C in a humidified atmosphere of 5% CO_2-95% air. Oocyte cultures were carried out in human tubal fluid (Irvine Scientific, Santa Ana, CA) supplemented with 0.5% BSA (fraction V; Gibco-BRL Life Technologies, Grand Island, NY). Culturing of oocytes was done in 0.1-ml drops of culture medium (10 oocytes/drop) under paraffin oil (Specialty Media, Phillipsburg, NJ), and cultures were incubated at 37°C in a humidified atmosphere of 5% CO_2-95% air. In some experiments, oocytes were incubated in the presence of an inhibitor of RAD51 (50 μM of 4,4′-diisothiocyanatostilbene-2,2′-disulfonic acid [DIDS-50]; product number D3514; Sigma) [47]. Oocyte morphology was evaluated at the end of the culture period.

Analysis of Apoptosis/Necrosis/Health

At the end of the culture period, some oocytes were fixed and evaluated as detailed previously [41, 48, 49] for characteristics of apoptosis, mainly morphological changes (e.g., condensation, budding, and cellular fragmentation) and biochemical alterations (i.e., DNA cleavage [Comet Assay kit; Trevigen, Gaithersburg, MD]; and cytochrome-*c* [cyt-*c*] release [InnoCyte cyt-*c* release kit; EMD Chemicals, Gibbstown, NJ]). Some other oocytes were used

for analysis of annexin V exposure (Apoptotic & Necrotic & Healthy cells quantification kit; Biotium, Inc., Hayward, CA), and caspase 3 (CASP3) activity (NucView 488; Biotium) following the manufacturer's instructions. The percentage of the total number of oocytes cultured per drop that underwent apoptosis in each experiment was then calculated.

Comet Assay

Pools of mature (MII) oocytes (bovine and mouse) were irradiated and then cultured for 6 h in control medium. DNA damage was assessed by the neutral version of the comet assay to detect DSBs, as detailed in the manufacturer's instructions (Trevigen) [42, 48, 49]. In this assay, damaged DNA is able to migrate from the cell during electrophoresis and can be visualized by using SYBR Green nucleic acid gel stain (Invitrogen; Carlsbad, CA). Cells that have accumulated DNA damage appear as fluorescent comets with tails of DNA fragmentation, whereas normal, undamaged DNA does not migrate far from the origin and remains inside the cell. The fluorescent tail length increases as a function of DNA damage. Analysis of the individual comets to generate quantitative data was performed using a computer-based program (VisComet; Impuls Computergestutzte Bildanalyse GmbH, Gilching, Germany) [50]. The program automatically calculates all measurement parameters including tail moments, tail percent intensity, and tail length. These parameters are widely regarded as the most informative measures of DNA damage. Here, we report tail percent intensity as percentage of damaged DNA per cell.

Cytochrome c Release

The analysis of cyt-*c* release is important in determining the cell's commitment to apoptosis. After irradiation, oocytes were fixed (8% paraformaldehyde in PBS), and the release of cyt-*c* was assessed with the InnoCyte cyt-*c* release kit (EMD Chemicals) according to the manufacturer's instructions. The kit reagent relies on the selective permeabilization of the cellular membrane for release of cytosolic components while leaving the mitochondrial membrane intact. Viable cells will display mitochondrial staining of cyt-*c*, while cells committed to the apoptotic process do not stain as they release cyt-*c* from the mitochondria to the cytosol. Cyt-c was detected using fluorescent microscopy after cells were stained with a monoclonal antibody specific to cyt-*c* and fluorescein isothiocyanate (FITC)-labeled secondary antibody.

Analysis of CASP3 Activity

Immediately after irradiation or at the end of the incubation period, oocytes were incubated for 1 h in the presence of 5 μl of NucView 488 CASP3 substrate solution, in accordance with manufacturer's instructions. In this assay, a specific CASP3 substrate is linked to a high-affinity DNA dye. The substrate rapidly crosses the cell membrane and enters the cell cytoplasm. If CASP3 is active, it cleaves the substrate, and therefore, the high-affinity DNA dye is released, which then binds and stains DNA (metaphase plate) bright green. The more the quantity of active CASP3 found in the cytoplasm, the larger the amount of DNA binding dye released and, therefore, the greater the amount of fluorescence [51]. At the end of that period, oocytes were fixed and analyzed with a fluorescent microscope using an FITC filter. Oocytes were serially scanned, and 10 optical sections were analyzed using MetaMorph software (Molecular Devices, Inc., Sunnyvale, CA). The total fluorescence was determined on stacked images, and mean relative fluorescent units (RFU) in each group were calculated for bovine or mouse oocytes.

Oocyte Microinjection

Immediately after they were isolated, denuded oocytes were microinjected with buffer or with recombinant human RAD51 (hRAD51; 6 pl of a 3.6 μg/μl stock per oocyte; this protein was purified and tested by Dr. Kurumizaka at RIKEN institute, Japan) or with mouse recombinant pro-CASP3 (6 pl of a 0.1 μg/μl stock; Biovision, Mountainview, CA) or with BSA (at equivalent concentrations). Oocytes that did not survive the microinjection procedure (usually <15%) were discarded [42, 48, 49]. Remaining oocytes were divided into two groups, control (CON) and irradiation exposed. Oocytes were cultured for up to 24 h with or without DIDS-50 μM. At the end of the culture period, assessment of apoptosis was performed as described earlier.

Immunodetection of RAD51 in Oocytes

Mature oocytes were isolated and cultured, either as unexposed (CON) or exposed to UV-B irradiation (100 microjoules). During the first 30 min of incubation, oocytes were fixed every 5 min and processed for detection of DNA (4′,6-diamidino-2-phenylindole [DAPI] staining) and colocalization of RAD51 by immunocytochemistry as described previously [41]. Briefly, at the end of the incubation period, oocytes were fixed in neutral-buffered 10% formalin for at least 20 min at room temperature. After fixation, oocytes were washed twice in PBS and stored at 4°C until the immunostaining procedure was performed. Permeabilization was achieved by a 10-min preexposure to 0.5% Triton X in PBS, followed by blocking in PBS containing 10% goat serum and 0.05% Triton X-100. Oocytes were then immunostained overnight at 4°C by using a 1:100 dilution of an affinity-purified mouse monoclonal antibody raised against full-length human RAD51 (Upstate USA, Inc., Charlottesville, VA) prepared in PBS supplemented with 0.05% Triton X-100. Slides were washed and incubated with a 1:1000 dilution of anti-mouse immunoglobulin G (IgG) conjugated with Alexa Red (Molecular Probes). Slides were washed, mounted with Prolong and subsequently viewed by confocal microscopy. Oocytes not exposed to primary antibody were used as negative controls to determine background, which was subtracted from each value before final analysis.

Quantitation of Fluorescent Signals

After they were stained for determination of CASP3 activity, cyt-*c* release, and RAD51 expression, oocytes were fixed (to fix the fluorescent signal) and transferred onto slides. The slides were washed and mounted with Prolong with or without DAPI (Invitrogen) and subsequently viewed by confocal microscopy. Oocytes were serially scanned, and 10 optical sections were analyzed using Metamorph software. Total fluorescence was determined with stacked images, and mean RFU values in each group were calculated for bovine or mouse oocytes. Oocytes not exposed to primary antibody or the substrate were used as negative controls to determine background, which was subtracted from each value before final analysis.

Statistical Analysis

Due to the high cost of performing experiments using NSCL facilities, samples were irradiated with Kr-78 only once, but all samples were run in triplicate. UV-B experiments were independently replicated at least 3 times. Quantitative data from the irradiated and unirradiated groups were subjected to one-way ANOVA, followed by the Duncan multiple range test or Scheffe F-test. A P value of less than 0.05 was considered significant for all comparisons. Data shown in graphs represent the means ± SEM of the combined data.

RESULTS

In previous experiments (our unpublished data) performed at Columbia University (NY), we bombarded mature (MII) and immature (germinal vesicle [GV]) mouse oocytes with alpha particles. In those preliminary observations, most oocytes exposed to alpha particles sustained DNA damage, characterized by DSBs, and died by apoptosis. In the present experiments, we tested the sensitivity of both bovine and mouse oocytes to irradiation by solar/cosmic particles, particularly to Kr-78 ions.

Based on morphology, we observed that within 6 h after LET irradiation, 82% of the mouse oocytes underwent necrosis (Fig. 2, H and I), while in the bovine oocytes, no apparent morphological changes were observed at that time (Fig. 2D). However, biochemical analyses revealed that from a total of 150 bovine oocytes analyzed, 21.3% ± 6.2% underwent necrosis, 25.3% ± 3.1% were healthy, and 53% ± 2.3% initiated an apoptotic program as determined by annexin-V-positive staining (Fig. 2, A and I). As for the mouse oocytes, this biochemical test confirmed that 82% ± 6.18% of oocytes were necrotic, 9.8% ± 3.08% were annexin-V positive, and 8.2% ± 1.23% were healthy (Fig. 2, E and I; N = 120). No apoptosis or necrosis was observed in the CON oocytes, i.e., those not subjected to LET radiation (bovine, N = 92; mouse, N = 40).

By 24 h postirradiation, the percentage of necrotic mouse oocytes had increased to 90% ± 4.67% (N = 60), whereas the percentage of bovine oocytes remained relatively constant, at approximately 23% ± 3.45% (N = 197). The percentage of annexin-V-positive bovine oocytes increased to 70% ± 3.81%. Neither apoptosis nor necrosis was seen in any of the control groups, either for mouse or bovine cells.

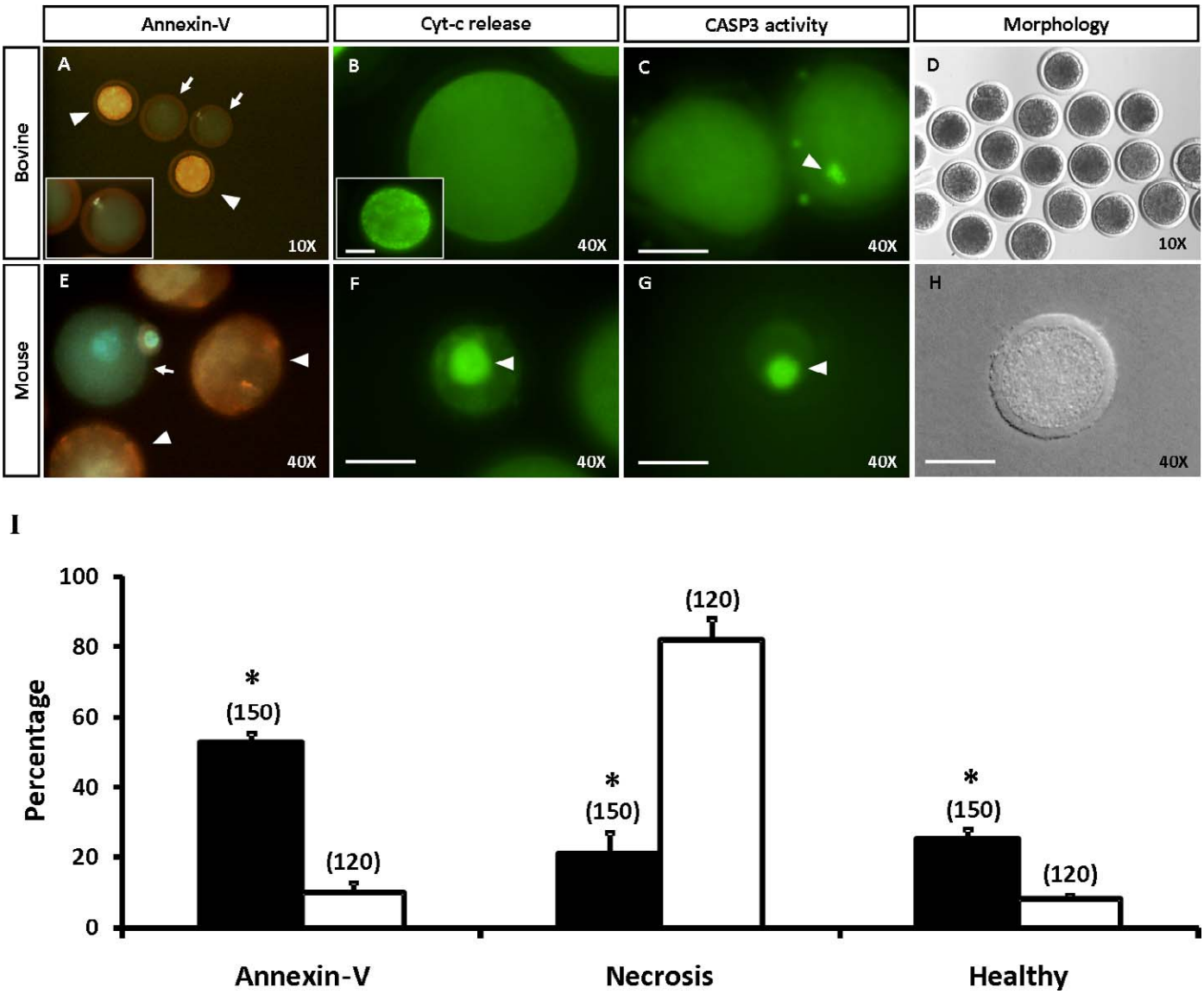

FIG. 2. Kr-78 irradiation initiates apoptosis in bovine oocytes but induces necrosis in mouse oocytes. Upon exposure to LET irradiation using Kr-78, bovine oocytes exhibited annexin-V exposure, cyt-*c* release, and activation of CASP3. **A**) annexin-V exposure, a marker of apoptosis, was detected via a fluorescein-labeled antibody. Positive oocytes (green) are indicated by arrows, whereas arrowheads point to necrotic oocytes (orange/red). During necrosis, the plasma membrane is damaged and therefore permeable to propidium iodide. The inset in **A** shows a higher magnification of one green oocyte shown in the main panel. **B**) Representative oocyte showing evidence of cyt-*c* release, shown by the homogenous green pattern (background color) all around the cytoplasm (more than 50% of bovine oocytes exhibited this pattern). Cells committed to the apoptotic process showed only this background color because they released cyt-*c* from the mitochondria to the cytosol and out of the cell. For comparison, the inset shows an oocyte where cyt-*c* release did not occur. These cells displayed staining of cyt-*c* inside the mitochondria, which is seen predominantly underneath the plasma membrane as a granular bright green staining. **C**) Caspase 3 activity, in this assay, a specific CASP3 substrate is linked to a high-affinity DNA dye. The substrate rapidly crosses the cell membrane and enters the cell cytoplasm. If CASP3 is active, it cleaves the substrate and therefore the high-affinity DNA dye is released, which then binds and stains the DNA (metaphase plate) brightly green. The greater the quantity of active CASP3 found in the cytoplasm, the larger the amount of DNA binding dye that is released and, therefore, the greater the amount of fluorescence. In the oocyte on the right, the arrowhead points to an area of positive reaction (bright green spot coinciding with the metaphase plate), whereas in the oocyte on the left, there is no activation of caspases (no bright spots seen, only green background). **D**) A group of bovine oocytes 6 h after irradiation. Morphologically, most oocytes shown here look normal (dark cytoplasm and no apparent abnormal morphological changes). Most mouse oocytes underwent necrosis, as indicated by propidium iodide-positive staining; no release of cyt-*c*; massive activation of CASP3; and necrotic morphological appearance. **E**) Arrowheads point to propidium iodide-positive oocytes. **F**) An example of a mouse oocyte in which the cyt-*c* remained inside the mitochondria, and therefore, it appears as a green bright spot. This spot most probably marks the area in the cytoplasm with aggregation of mitochondria. When the oocytes release the cyt-*c* from the mitochondria after treatment (as was the case in bovine oocytes after irradiation), no bright spots are detected; only 10% of mouse oocytes released cyt-*c* following irradiation. **G**) Massive activation of CASP3 was seen in 80% of the mouse oocytes. Notice that the bright green fluorescence occupies approximately one fourth of the cytoplasm (compare with Fig. 2C, where only a small green spot is detected). **H**) Characteristic morphology of a necrotic mouse oocyte as seen with light microscopy 6 h after irradiation. During necrosis, the oocytes flatten, the perivitelline space disappears due to the expansion of the oocyte cytoplasm, and the oocyte cytoplasm becomes very translucent; there is no cellular fragmentation because there is a lack of ATP. Bars = 80 μm. **I**) Quantitative data show the mean percentages ± SEM of healthy, apoptotic (annexin-V-positive) and necrotic bovine and mouse oocytes following exposure to Kr-78 irradiation. No apoptosis or necrosis was observed in the control oocytes (bovine, N = 92; mouse, N = 40). Filled bars, bovine; opened bars, mouse. The number of oocytes analyzed per group is indicated at the top of the bars. $^*P < 0.05$. All photomicrographs and quantitative data presented were obtained 6 h after irradiation.

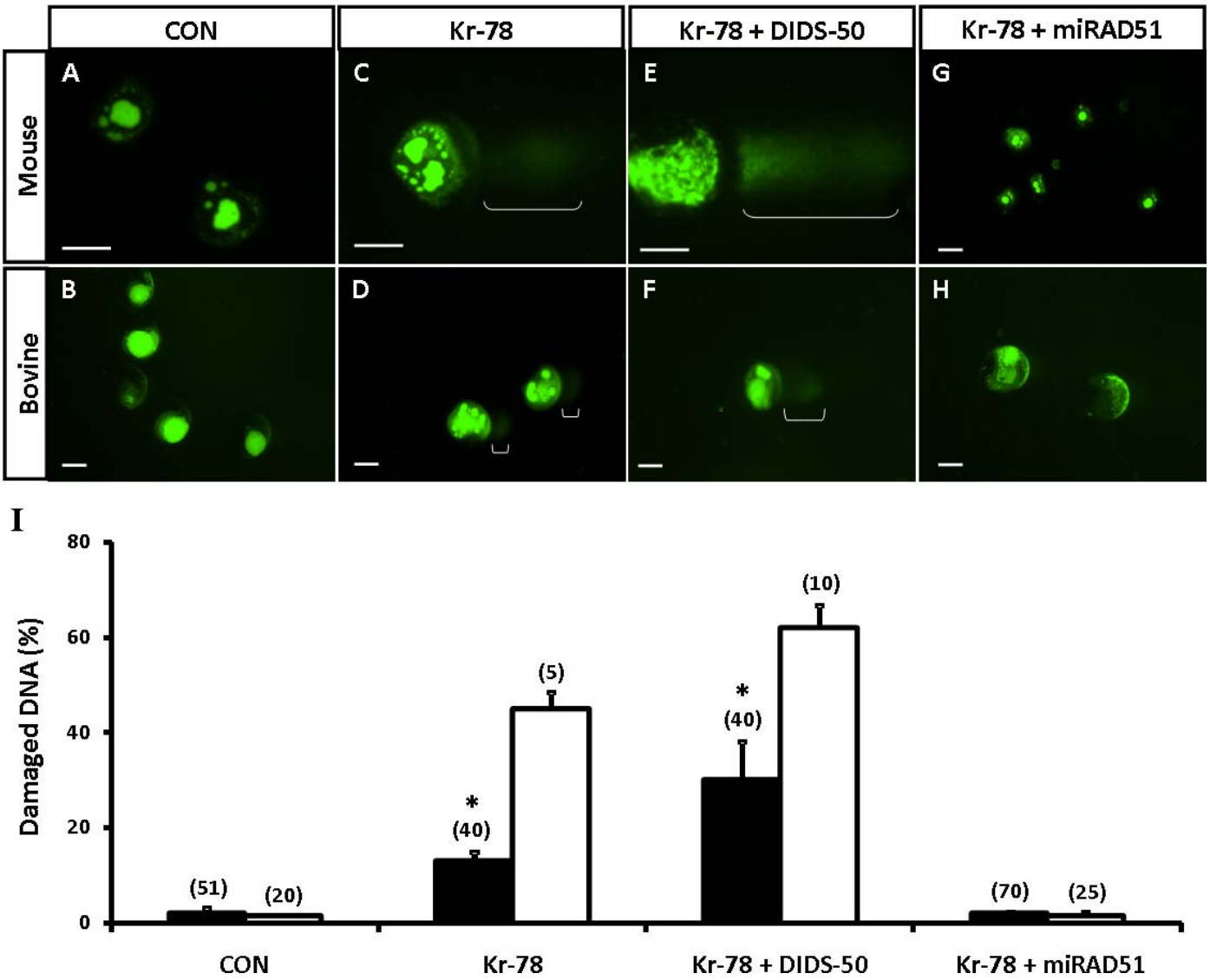

FIG. 3. Kr-78 irradiation induces DNA damage in both bovine and mouse oocytes. DNA damage was evaluated by the comet assay. In this assay, damaged DNA is able to migrate out of the cell during electrophoresis and can be visualized using SYBR Green nucleic acid gel stain. Cells that have accumulated DNA damage appear as fluorescent comets with tails of DNA fragmentation (in **C**–**F**, comets are marked by brackets), whereas, normal undamaged DNA does not migrate far from the origin and remains inside the cell (**A**, **B**, **G**, and **H**). The fluorescent tail length increases as a function of DNA damage. **A** and **B**) No DNA damage was observed in oocytes that were not exposed to irradiation. **C** and **D**) Mouse and bovine oocytes exposed to irradiation exhibit DNA damage. In the bovine oocyte (**D**) the percentage of damaged DNA was three times less than in the mouse oocyte (**C**). **E** and **F**) Inhibition of RAD51 with DIDS-50 (50 μM) following irradiation increased the percentage of damaged DNA in both mouse and bovine oocytes. **G** and **H**) Microinjection of recombinant hRAD51 before irradiation, totally prevented irradiation-induced DNA damage in both bovine and mouse oocytes. Original magnification ×40 (**A**, **C**, **E**) and ×10 (**B**, **D**, **F**–**H**); bars = 80 μm. **I**) Quantitation of the DNA damage shows the mean percentages ± SEM of damaged DNA under different conditions. Filled bars, bovine; opened bars, mouse. The number of oocytes analyzed per group is indicated at the top of the bars. $^*P < 0.05$.

Interestingly, although a high percentage of bovine oocytes were annexin-V positive (an early marker of apoptosis), by 6 h after irradiation, we never observed cytoplasmic fragmentation, even after 24 h of incubation. Therefore, to determine whether the apoptotic program in the bovine oocyte does or does not progress beyond the earlier stages, we analyzed three downstream apoptotic events, cyt-*c* release, CASP3 activity, and DNA damage, in both bovine and mouse oocytes at 6 h and at 24 h after irradiation. Consistent with the earlier findings of necrosis in mouse oocytes, the mouse germ cells exhibited extensive activation of CASP3 (Fig. 2G) and no release of cyt-*c* (Fig. 2F), both findings reflecting death by necrosis. From the 50 mouse oocytes analyzed (25 oocytes at 6 h and 25 oocytes at 24 h) only 5 oocytes exhibited cyt-*c* release (data not shown). Moreover, 40 of the 50 oocytes analyzed displayed extensive activation of CASP3 (RFU, 640 ± 58; $P < 0.05$ compared to bovine) (Fig. 2G). On the other hand, more than 50% of bovine oocytes exhibited cyt-*c* release (54% ± 2.36%) (Fig. 2B) and mild activation of CASP3 (RFU, 124 ± 23) (Fig. 2C), confirming the fact that apoptosis was underway. No activation of CASP3 was noted in control oocytes; the fluorescent signal remained at approximately background levels for both mouse and bovine oocytes (RFUs of 26 ± 4.9 and 48 ± 1.6, respectively). Very few oocytes (<1%) released cyt-*c* in the control groups from both mouse and bovine oocytes.

Next, we analyzed DNA damage by using the comet assay. It is important to remember that necrotic oocytes do not form any comet, and therefore, comparison between bovine and mouse oocytes was performed using a low number of mouse

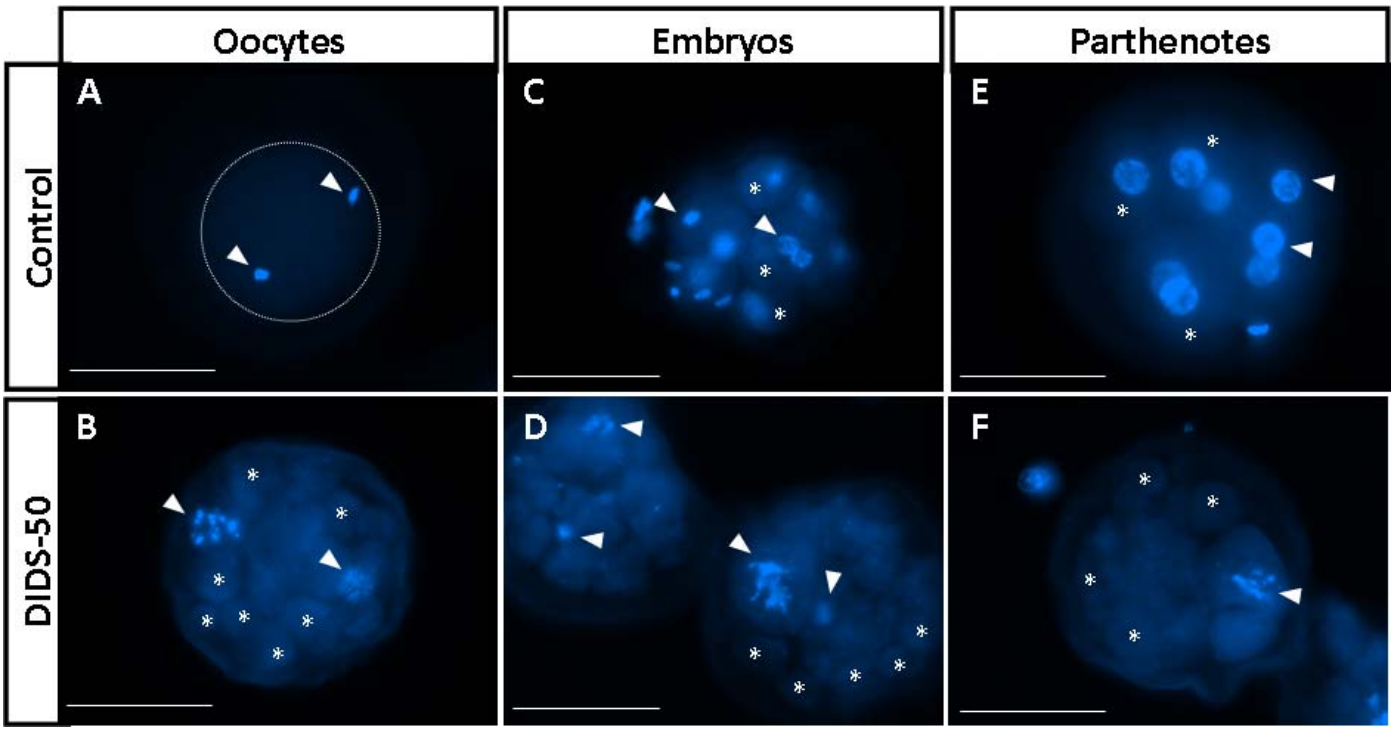

FIG. 4. Inhibition of RAD51 induces both DNA and cellular fragmentation in meiotic cells (oocytes) and mitotic cells (blastomeres). Bovine oocytes, IVF embryos, and parthenotes were incubated with or without DIDS-50 for 24 h and then fixed and stained with DAPI. **A**) Intact DNA in the control oocyte is seen as two bright spots showing the DNA in the metaphase plate and in the polar body (arrowheads). The oocyte cytoplasm is intact, with no evidence of cytoplasmic fragmentation (dotted lines around the cytoplasm). **B**) Oocytes treated with DIDS-50, fragmented DNA (arrowheads) is seen inside some cytoplasmic fragments. Only one of the fragments containing cleaved DNA is in focus. Cellular fragmentation is evident by the presence of multiple cytoplasmic fragments (some of the fragments are labeled with asterisks); compare this oocyte with the control oocyte shown in **A**. **C** and **E**) Respectively, IVF embryos and parthenote controls show the typical appearance of mitotic DNA (arrowheads) inside blastomeres (limited number of cells of approximately equal size; some labeled with asterisks); compare to **D** and **F,** where embryos and parthenotes were treated with DIDS-50; multiple cytoplasmic fragments (cytoplasmic fragmentation; asterisks) of various sizes some of them containing fragmented DNA (arrowheads) are apparent. Original magnification ×40; bars = 80 μm.

oocytes. The results showed that 50% of bovine oocytes sustained DNA damage, but the extent of damaged DNA was 3 times less than the damage displayed by mouse oocytes undergoing apoptosis (respectively, percentage of damaged DNA, 15% ± 5% [N = 40] vs. 45% ± 3.6% [N = 5] (Fig. 3, D and I, and C and I, respectively). Taken together, these results provide evidence that after irradiation, the bovine oocyte starts the apoptotic cell death program, but the program appears to stop short of cytoplasmic fragmentation.

Next, to explore the mechanism(s) leading to the halted cell death program, we targeted two pathways, DNA repair and CASP3 activation. Both pathways have been proven to play critical roles in the induction of cytoplasmic fragmentation in other experimental models [42, 52–54]. Recently, we demonstrated that in mouse oocytes, overexpression of RAD51 prevents DNA damage and cytoplasmic fragmentation [41, 42]. Hence, to start elucidating the significance of RAD51 in bovine oocytes, we first inhibited its activity by incubating nonirradiated bovine oocytes for 24 h with or without DIDS-50 (a specific inhibitor of RAD51). Inhibition of RAD51 alone induced 33% ± 3.5% cellular fragmentation (N = 50) (Fig. 4B), whereas 0% cellular fragmentation was found in both control (CON, no DIDS; N = 50) (Fig. 4A) and irradiation alone (Kr-78; N = 46). However, when bovine oocytes were first irradiated and then incubated in the presence of DIDS-50 for 24 h, the percentage of fragmented oocytes increased to 47% ± 1.89% (using Kr-78 plus DIDS-50; N = 45), and the amount of damaged DNA increased as well (percentage of damaged DNA, 30% ± 8%; N = 40) (Fig. 3, F and I) compared to oocytes exposed to Kr-78 alone (percentage of damaged DNA, 13% ± 2%; N = 40) (Fig. 3, D and I) or no DIDS CON (percentage of damaged DNA, 2.0% ± 0.97%; N = 51) (Fig. 3, B and I). In mouse oocytes, inhibition of RAD51 following irradiation increased the percentage of damaged DNA from 45% ± 3.6% (using Kr-78 irradiation; N = 5) (Fig. 3, C and I) to 62% ± 4.7% (using Kr-78 plus DIDS-50; N = 10) (Fig. 3, E and I).

In contrast, microinjection of recombinant hRAD51 before irradiation totally prevented irradiation-induced DNA damage in both bovine and mouse oocytes (using microinjected RAD51 plus Kr-78, the percentage of damaged DNA in bovine was 2% ± 0.23% [N = 70], whereas in mouse, the percentage of damaged DNA was 1.5% ± 0.64% [N = 25]) (Fig. 3, H and I, and G and I, respectively).

Therefore, in bovine and mouse oocytes, RAD51 appears to be a critical player during both the response to DNA damage and in the final steps of apoptosis culminating in cytoplasmic fragmentation. However, because the mature oocyte is a cell that is destined to die in the absence of fertilization, questions may arise as to whether the effects we observed after inhibiting RAD51 are applicable to other cells, particularly actively dividing cells. Therefore, we evaluated the effects of incubating bovine IVF embryos and parthenotes at the zygote stage for 24 h with or without DIDS-50. For both IVF embryos and parthenotes, incubation with DIDS-50 for 24 h induced cytoplasmic fragmentation (83% ± 5.12% for IVF [N = 106]; 67.8% ± 11.02% for parthenotes [N = 169]; $P = 0.26$) (Fig. 4, D and F, respectively) significantly more ($P < 0.05$)

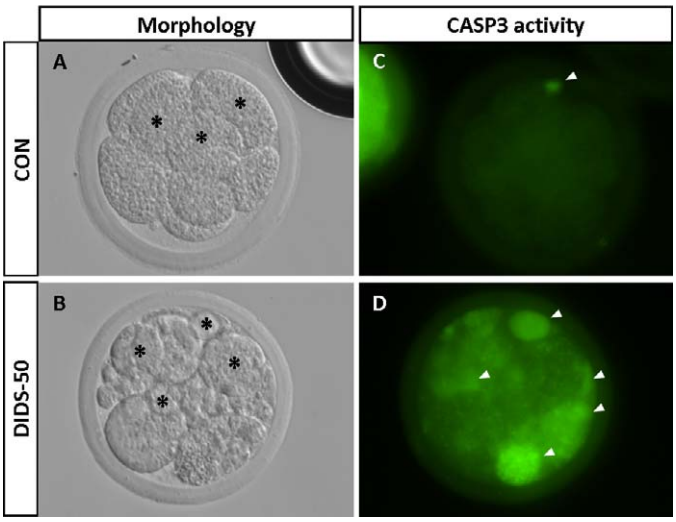

FIG. 5. Bovine embryos exposed to DIDS-50 exhibited increased cellular fragmentation and increased activation of CASP3. IVF embryos were treated at the zygote stage and incubated for 24 h without (**A** and **C**) or with DIDS-50 (**B** and **D**). At the end of the incubation period, the embryos were stained for the presence of active CASP3 (Fig. 2 legend describes this assay). **A**) Control embryo contains blastomeres (some of them denoted by asterisks) of approximately equal size and lack of cytoplasmic fragments. **B**) Treated embryo exhibits cytoplasmic fragmentation characterized by the presence of cytoplasmic fragments of different sizes (some of them marked with asterisks). **C**) Caspase 3 activity was not detected in the control embryo (homogenous green background); only a small positive spot is seen (bright green; arrowhead), most probably corresponding to the second polar body. **D**) The embryo treated with DIDS-50 exhibits several of the fragments positive for CASP3 activity, as shown by the bright green spots (arrowheads). Compare these results to the CASP3 activity seen in bovine oocytes following irradiation (Fig. 2C). Original magnification ×60.

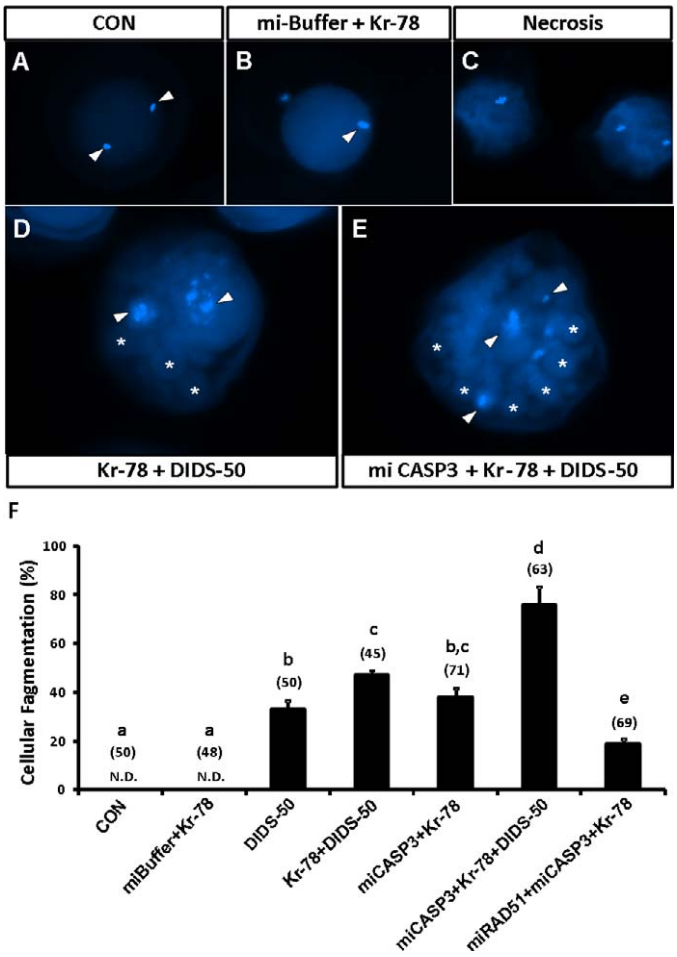

FIG. 6. Lack of cellular fragmentation in the bovine oocyte following irradiation might be due to mild activation of CASP3. **A–E**) DAPI staining of the oocytes under different experimental conditions. **A**) Control oocyte, no DNA cleavage and no cytoplasmic fragmentation. Intact DNA (arrowheads) is observed; one of those corresponds to the DNA of the oocyte (metaphase plate) and the other to the DNA in the polar body. **B**) Notice that DNA damage induced by Kr-78 radiation is not detected by DAPI staining, and the DNA appears to be intact (arrowhead); compare to Figure 3D. **C**) Examples of necrotic oocytes found shortly after microinjection. Notice that there is neither DNA cleavage nor cytoplasmic fragmentation. **D**) Cellular and DNA fragmentation (denoted, respectively, by asterisks and arrowheads) in bovine oocytes exposed to radiation and incubated in the presence of an inhibitor of RAD51. **E**) Maximum cellular and DNA fragmentation (denoted, respectively, by asterisks and arrowheads) were observed when bovine oocytes were treated with a combination of microinjected CASP3 plus Kr-78 plus DIDS-50. Original magnification ×40 (**A**–**C**) and ×60 (**D**, **E**). **F**) Quantitative analysis of cellular fragmentation for different treatment groups (means ± SEM). Microinjection of bovine oocytes with hRAD51 markedly decreased cytoplasmic fragmentation induced by CASP3 plus Kr-78. The number of oocytes analyzed per group is shown at the top of each bar. Columns with different letters are significantly different. $P < 0.05$.

than the cellular fragmentation in control IVF embryos (1.03% ± 1.03% [N = 138]) (Fig. 4C) or in control parthenotes (1.5% ± 1.04% [N = 143]) (Fig. 4E). In addition to increased cellular fragmentation, embryos exposed to DIDS-50 for 24 h also exhibited increased activation of CASP3 (RFU, 532 ± 15 for IVF [N = 64]; RFU, 487 ± 24 for parthenotes) (Fig. 5D) compared to the CASP3 activity seen in control embryos (RFU, 53 ± 5.2 [N = 78]; $P < 0.05$) (Fig. 5C) or in oocytes following irradiation (RFU, 124 ± 23 [N = 50]; $P < 0.05$) (Fig. 2C).

Caspase 3 has been implicated in cytoplasmic fragmentation in other cells [52–54], and as the bovine oocyte exhibited mild activation of CASP3 following irradiation, our next step was to increase CASP3 activity in bovine oocytes by microinjecting recombinant CASP3 before exposing the oocytes to irradiation. Microinjection of CASP3 induced cellular fragmentation without significant changes in DNA damage (microinjected CASP3 plus Kr-78, 38% ± 3.7% cellular fragmentation [N = 71]; $P < 0.05$) (Fig. 6F) compared to control (CON, 0% cellular fragmentation) (Fig. 6, A and F) or irradiation with Kr-78 (0% cellular fragmentation) (Fig. 6, B and F) or UV-B alone (0% cellular fragmentation). The maximum cellular fragmentation was observed when oocytes were treated with a combination of microinjected CASP3 followed by irradiation and then incubated in the presence of DIDS-50 (76% ± 7.2% cellular fragmentation [N = 63]; $P < 0.05$) (Fig. 6, E and F). Importantly, microinjection of bovine oocytes with hRAD51 markedly decreased both cytoplasmic fragmentation (19% ± 2.1% cellular fragmentation [N = 69]) (Fig. 6F) and DNA damage (data not shown) induced by microinjected CASP3 plus Kr-78 ($P < 0.05$).

In earlier experiments, we found that bovine oocytes do die if exposed to UV-B irradiations; nevertheless, they do not undergo cellular fragmentation, an outcome that closely resembles the results observed following their exposure to Kr-78. Also, because UV-B waves are also components of solar/cosmic radiation, we decided to use their energy to further analyze the mechanism underlying the lack of cellular fragmentation in bovine oocytes. Hence, in the last set of

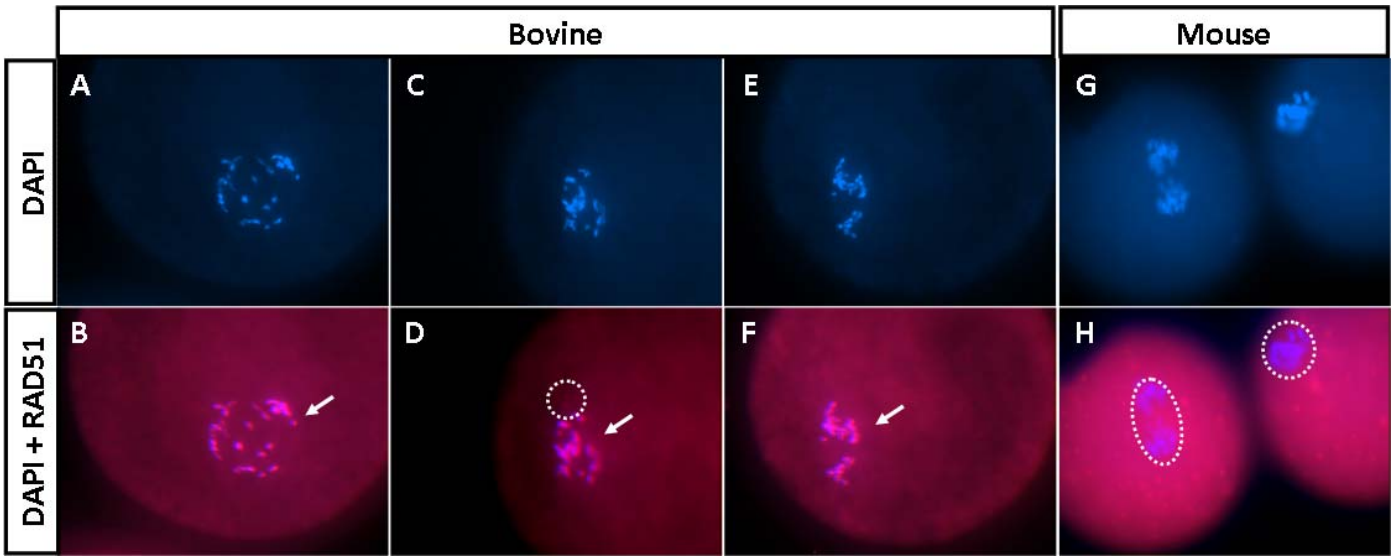

FIG. 7. Following induction of DNA damage, the RAD51 response occurs faster in bovine oocytes than in mouse oocytes. **A**–**F**) Five minutes after irradiation, most bovine oocytes (three oocytes shown) showed evidence of RAD51 colocalization to the damaged DNA (white arrows). The dotted area in **D** points to RAD51 localized close by the DNA but without colocalization. **G** and **H**) No evidence of colocalization of the protein in mouse oocytes (two shown) during the first 10 min. However, by 15 min, the colocalization was apparent in 50% of the oocytes analyzed (data not shown). The dotted areas in **H** point to the DNA of the oocytes. Original magnification ×60 (**A**–**F**) and ×100 (**G** and **H**).

experiments, we analyzed the location of RAD51 by immunocytochemistry every 5 min, during the first 15 min following UV-B irradiation in both bovine and mouse oocytes. We found that upon induction of DNA damage, the RAD51 response was faster in bovine oocytes than in mouse oocytes. Five minutes after irradiation, 84% of bovine oocytes (N = 46) showed evidence of RAD51 colocalization to the damaged DNA (Fig. 7, A–F), with no apparent change for the next 10 min (N = 98). In contrast, we found no evidence of colocalization of the protein in mouse oocytes during the first 10 min (N = 100) (Fig. 7, G and H). However, by 15 min, the colocalization was apparent in 50% of the mouse oocytes analyzed (N = 50; data not shown) [41].

DISCUSSION

Based on comparisons between mouse and bovine oocytes, data from the present experiments suggest that large differences in radiation sensitivity exist between female germ cells from different mammalian species. The apparent resistance of bovine oocytes to ionizing radiation could be explained as an adaptive response to continuous exposure [7, 55–59]; after all, even before domestication, livestock have been grazing natural rangelands under direct sun rays and being bombarded by solar/cosmic radiations. These energy correlates are not limited to livestock, as all living organisms are continuously exposed to natural ionizing radiation. Hence, it is generally accepted that evolution of life on our planet has been relatively influenced by mutagenic effects of irradiants that reach the earth [6]. In the present studies, we uncovered the fact that mouse oocytes are extremely sensitive to radiation compared to bovine oocytes, confirming the concept that the degree of resistance to radiation appears to be inversely correlated to the expanse of earlier exposures. Similarly in humans, as suggested recently by Astbury [23], there is a lack of direct relationship between death rates from cancer and the intensity of CRs, when comparing data from people living at high altitudes to those living at sea level; most probably this reflects the body's adaptation mechanism(s) for defense against cellular damage in increased radiation fields.

Recent evidence indicates that different cells exposed to low doses of ionizing radiation switched on the transient up-regulation of DNA repair systems and antioxidant activity in a phenomenon called adaptive response [55–60]. However, this adaptive response also has been associated with early activation of DNA repair mechanisms lacking repair fidelity, which possibly contribute to an accumulation of chromosomal aberrations [61, 62]. Therefore, in the bovine oocyte, the early activation of such faulty DNA repair mechanisms following a DNA insult might directly contribute to infertility. Although in the present experiments we did not evaluate fertilizability and embryo development of the oocytes exposed to radiation, our recent unpublished observations are that bovine oocytes exposed to a DNA-damaging agent (doxorubicin) are fertilizable; however, further preimplantation embryo development is highly compromised. Consequently, we speculate that bovine oocytes bearing aberrant repairs are fertilizable, even though the ensuing embryos undergo fetal/perinatal death, thus affecting the overall fertility of cattle.

Earlier studies in humans have observed unique patterns of DNA damage and gene expression following exposure to high LET radiation [39, 63]. However, the mechanism(s) responsible for the alterations in gene expression remains mostly unknown. It is our hypothesis that global epigenetic transformations of the genome that particularly affects genes involved in the DNA damage response (among those, the RAD51 gene) have evolved in bovine oocytes as a strategy to adapt to continuous irradiation by secondary solar/cosmic particles and that such adaptations play an important role in the development of infertility. Additional studies will be required to understand the regulation of RAD51 at the molecular level in the bovine model.

Several questions remain unanswered; for example, what controls the speed of DNA damage recognition in the bovine compared to that in the mouse; and why do meiotic cells (oocytes) appear to be less sensitive to inhibition of RAD51 actions than mitotic cells (blastomeres)? It would be even more intriguing to determine what purpose is served to maintain cells that are halfway dead. Is this to control and maintain a constant

rate of germ cell demise and, therefore, to prevent acceleration of germ cell depletion and shortening of the reproductive life [64–66]; or is its purpose to prevent a massive immune response, because apoptosis has the potential of inducing or exacerbating autoreactive immune responses by exposing the cell's nuclear antigens [67–71]? Moreover, mitochondrial injury and activation of the DNA damage/repair pathways also trigger the release of endogenous damage-associated molecular patterns that activate innate immunity through pattern recognition receptors [72].

Interestingly, in the bovine oocyte, as happens in many other types of cells, CASP3 is required for both cytoplasmic (membrane blebbing and fragmentation) and nuclear events (DNA fragmentation) associated with apoptosis [52–54]. However, in the mouse oocyte, CASP3 is dispensable for either one of these apoptotic events [73]. Therefore, continued studies of the effects of and mechanisms involved in radiation on different mammalian models would be justified in order to delineate the potential risks associated with exposure of women to radiation.

Although knowledge regarding the impact of solar CRs on the health of airplane crews has been growing [2–4, 74–77], our scientific knowledge of approximate health effects of natural ionizing radiation exposure at ground level on plants, animals, and humans remain largely undetermined. Here we tested the direct effects of ionizing radiation on oocytes. Although the results are significant and open new areas of research, we believe that efforts should also be directed toward the study of radiation-induced bystander effects (RIBE), which are radiation-like inductions in cells that have not been irradiated [18–20]. RIBE is a novel phenomenon, which indicates that at low irradiation doses, pathophysiologic effects triggered via cell signaling are more important than direct DNA damage. Some of these studies have shown that, at low levels of exposure, the transport of bioactive substances from irradiated to unirradiated ''bystander'' cells can even amplify the damage. In preliminary studies, we have observed that while mouse oocytes exposed to direct irradiation (alpha particles) die by apoptosis, oocytes exposed to irradiated oocytes (indirect exposure) die by necrosis. This suggests a more aggressive insult, probably due to amplification of the initial signal. Hence, the growing realization that cell signaling can trigger important inductions in bystanders opens up several potential therapeutic strategies that could effectively protect animals and humans against solar/cosmic radiation-induced infertility; it is imperative to determine the potential hazard of RIBE in oocytes.

Bovine oocytes appear to be capable of surviving for relatively long periods after exposure to high-LET radiation. The persistence of these damaged cells may have implications not only for livestock production but also for characterizing long-term health risks associated with human activity in space. We are aware, however, that results obtained from the present experiments are for one cell type only and may or may not accurately reflect the induction and persistence of damage in other tissues. As such, additional studies would be necessary to obtain refined statistical estimates of the damage in various tissues at multiple times after exposure. Additionally, it is important to factor in the type of cosmic particles (primary or secondary) to be used in future experiments, because, as we pointed out in the introduction, we used Kr-78 radiation, which may be negligible in the secondary cosmic flux.

ACKNOWLEDGMENT

We thank the director and staff of the NSCL for their help during conception and development of this project.

REFERENCES

1. Chen J, Chenette D, Clark R, Garcia-Munoz M, Guzik TG, Pyle KR, Sang Y, Wefel JP. A model of galactic cosmic rays for use in calculating linear energy transfer spectra. Adv Space Res 1994; 14:765–769.
2. Chen J, Lewis BJ, Bennett LG, Green AR, Tracy BL. Estimated neutron dose to embryo and foetus during commercial flight. Radiat Prot Dosimetry 2005; 114:475–480.
3. Chen J, Mares V. Significant impact on effective doses received during commercial flights calculated using the new ICRP radiation weighting factors. Health Phys 2010; 98:74–76.
4. Chen J, Mares V. Estimate of doses to the fetus during commercial flights. Health Phys 2008; 95:407–412.
5. Chen J, Timmins R, Verdecchia K, Sato T. An estimation of Canadian population exposure to cosmic rays. Radiat Environ Biophys 2009; 48:317–322.
6. Ferrari F, Szuszkiewicz E. Cosmic rays: a review for astrobiologists. Astrobiology 2009; 9:413–436.
7. Held KD. Effects of low fluences of radiations found in space on cellular systems. Int J Radiat Biol 2009; 85:379–390.
8. Dorman LI. Cosmic Rays in the Earth's Atmosphere and Underground. Norwell, MA: Kluwer Academic Publishers; 2004.
9. US Environmental Protection Agency. *Radiation Risks And Realities*. Washington, DC: US Environmental Protection Agency; 2007. World Wide Web (URL: epa.gov/radiation/docs/402-k-07-006.pdf).
10. Goldman M. Ionizing radiation and its risks. West J Med 1982; 137:540–547.
11. Shimada A, Shima A, Nojima K, Seino Y, Setlow RB. Germ cell mutagenesis in medaka fish after exposures to high-energy cosmic ray nuclei: a human model. Proc Natl Acad Sci U S A 2005; 102:6063–6067.
12. Muller HJ. Genetic damage produced by radiation. Science 1955; 122:759.
13. Yang TC, Mei M, George KA, Craise LM. DNA damage and repair in oncogenic transformation by heavy ion radiation. Adv Space Res 1996; 18:149–158.
14. Arenz A, Hellweg CE, Meier MM, Baumstark-Khan C. Gene expression in mammalian cells after exposure to 95 MeV/amu argon ions. Adv Space Res 2005; 36:1680–1688.
15. Lau P, Baumstark-Khan C, Hellweg CE, Reitz G. X-irradiation-induced cell cycle delay and DNA double-strand breaks in the murine osteoblastic cell line OCT-1. Radiat Environ Biophys 2010; 49:271–280.
16. Baumstark-Khan C, Heilmann J, Rink H. Induction and repair of DNA strand breaks in bovine lens epithelial cells after high LET irradiation. Adv Space Res 2003; 31:1583–1591.
17. Todd P, Pecaut MJ, Fleshner M. Combined effects of space flight factors and radiation on humans. Mutat Res 1999; 430:211–219.
18. Mothersill C, Seymour C. Radiation-induced bystander effects: evidence for an adaptive response to low dose exposures? Dose Response 2006; 4:283–290.
19. Mothersill C, Seymour C. Radiation-induced bystander and other non-targeted effects: novel intervention points in cancer therapy? Curr Cancer Drug Targets 2006; 6:447–454.
20. Zhang Y, Zhou J, Baldwin J, Held KD, Prise KM, Redmond RW, Liber HL. Ionizing radiation-induced bystander mutagenesis and adaptation: quantitative and temporal aspects. Mutat Res 2009; 671:20–25.
21. Brenner DJ, Elliston CD. The potential impact of bystander effects on radiation risks in a Mars mission. Radiat Res 2001; 156:612–617.
22. Stoupel E. Cardiac arrhythmia and geomagnetic activity. Indian Pacing Electrophysiol J 2006; 6:49–53.
23. Astbury A. Is there a link between cancer and cosmic rays? TRI-PP-00-33. Vancouver, BC; 2000. World Wide Web (URL: legacyweb.triumf.ca/publications/pub/arch00/pp-00-33.ps).
24. Badrinath P, Ramaiah S. Risk of breast cancer among female airline cabin attendants. Findings may have been due to exposure to cosmic radiation or recall bias. BMJ 1999; 318:125.
25. Pukkala E, Aspholm R, Auvinen A, Eliasch H, Gundestrup M, Haldorsen T, Hammar N, Hrafnkelsson J, Kyyronen P, Linnersjo A, Rafnsson V, Storm H, et al. Incidence of cancer among Nordic airline pilots over five decades: occupational cohort study. BMJ 2002; 325:567.
26. Vitzthum VJ. The home team advantage: reproduction in women indigenous to high altitude. J Exp Biol 2001; 204:3141–3150.
27. Shamir L. Does cosmic weather affect infant mortality rate? J Environ Health 2010; 73:20–23.
28. Luo Y, Liao W, Chen Y, Cui J, Liu F, Jiang C, Gao W, Gao Y. Altitude can alter the mtDNA copy number and nDNA integrity in sperm. J Assist Reprod Genet 2011; 28:951–956.
29. Sigl G, Schramm DN, Lee S, Hill CT. Implications of a possible clustering

of highest-energy cosmic rays. Proc Natl Acad Sci U S A 1997; 94:10501–10505.
30. Haynes CV Jr, Boerner J, Domanik K, Lauretta D, Ballenger J, Goreva J. The Murray Springs Clovis site, Pleistocene extinction, and the question of extraterrestrial impact. Proc Natl Acad Sci U S A 2010; 107:4010–4015.
31. Crutzen PJ, Bruhl C. Mass extinctions and supernova explosions. Proc Natl Acad Sci U S A 1996; 93:1582–1584.
32. Gallet Y, Genevey A, Le Goff M, Fluteau F, Eshraghi SA. Possible impact of the Earth's magnetic field on the history of ancient civilizations. Earth Planet Sci Lett 2006; 246:17–26.
33. Kuhne WW, Gersey BB, Wilkins R, Wu H, Wender SA, George V, Dynan WS. Biological effects of high-energy neutrons measured in vivo using a vertebrate model. Radiat Res 2009; 172:473–480.
34. Blaustein AR, Belden LK. Amphibian defenses against ultraviolet-B radiation. Evol Dev 2003; 5:89–97.
35. Foster WG. Environmental toxicants and human fertility. Minerva Ginecol 2003; 55:451–457.
36. Giudice LC. Infertility and the environment: the medical context. Semin Reprod Med 2006; 24:129–133.
37. Royal M, Mann GE, Flint AP. Strategies for reversing the trend towards subfertility in dairy cattle. Vet J 2000; 160:53–60.
38. Nir Markusfeld O. What are production diseases, and how do we manage them? Acta Vet Scand Suppl 2003; 98:21–32.
39. Nelson GA. Fundamental space radiobiology. Gravit Space Biol Bull 2003; 16:29–36.
40. Fahrudin M, Otoi T, Karja NW, Mori M, Murakami M, Suzuki T. Analysis of DNA fragmentation in bovine somatic nuclear transfer embryos using TUNEL. Reproduction 2002; 124:813–819.
41. Kujjo LL, Laine T, Pereira RJ, Kagawa W, Kurumizaka H, Yokoyama S, Perez GI. Enhancing survival of mouse oocytes following chemotherapy or aging by targeting Bax and Rad51. PLoS One 2010; 5:e9204.
42. Perez GI, Acton BM, Jurisicova A, Perkins GA, White A, Brown J, Trbovich AM, Kim MR, Fissore R, Xu J, Ahmady A, D'Estaing SG, et al. Genetic variance modifies apoptosis susceptibility in mature oocytes via alterations in DNA repair capacity and mitochondrial ultrastructure. Cell Death Differ 2007; 14:524–533.
43. Kuznetsov S, Pellegrini M, Shuda K, Fernandez-Capetillo O, Liu Y, Martin BK, Burkett S, Southon E, Pati D, Tessarollo L, West SC, Donovan PJ, et al. RAD51C deficiency in mice results in early prophase I arrest in males and sister chromatid separation at metaphase II in females. J Cell Biol 2007; 176:581–592.
44. Adamczyk A, Clowdsley M, Qualls G, Blattnig S, Lee K, Fry D, Stoffle N, Simonsen L, Slaba T, Walker S, Zapp E. Full mission astronaut radiation exposure assessments for long duration lunar surface missions. IEEE 2011; 1–15.
45. Parrish JJ, Susko-Parrish JL, Leibfried-Rutledge ML, Critser ES, Eyestone WH, First NL. Bovine in vitro fertilization with frozen-thawed semen. Theriogenology 1986; 25:591–600.
46. Susko-Parrish JL, Leibfried-Rutledge ML, Northey DL, Schutzkus V, First NL. Inhibition of protein kinases after an induced calcium transient causes transition of bovine oocytes to embryonic cycles without meiotic completion. Dev Biol 1994; 166:729–739.
47. Ishida T, Takizawa Y, Kainuma T, Inoue J, Mikawa T, Shibata T, Suzuki H, Tashiro S, Kurumizaka H. DIDS, a chemical compound that inhibits RAD51-mediated homologous pairing and strand exchange. Nucleic Acids Res 2009; 37:3367–3376.
48. Jurisicova A, Lee HJ, D'Estaing SG, Tilly J, Perez GI. Molecular requirements for doxorubicin-mediated death in murine oocytes. Cell Death Differ 2006; 13:1466–1474.
49. Perez GI, Jurisicova A, Matikainen T, Moriyama T, Kim MR, Takai Y, Pru JK, Kolesnick RN, Tilly JL. A central role for ceramide in the age-related acceleration of apoptosis in the female germline. FASEB J 2005; 19:860–862.
50. Duty SM, Singh NP, Silva MJ, Barr DB, Brock JW, Ryan L, Herrick RF, Christiani DC, Hauser R. The relationship between environmental exposures to phthalates and DNA damage in human sperm using the neutral comet assay. Environ Health Perspect 2003; 111:1164–1169.
51. Takai Y, Matikainen T, Jurisicova A, Kim MR, Trbovich AM, Fujita E, Nakagawa T, Lemmers B, Flavell RA, Hakem R, Momoi T, Yuan J, et al. Caspase-12 compensates for lack of caspase-2 and caspase-3 in female germ cells. Apoptosis 2007; 12:791–800.
52. Janicke RU, Sprengart ML, Wati MR, Porter AG. Caspase-3 is required for DNA fragmentation and morphological changes associated with apoptosis. J Biol Chem 1998; 273:9357–9360.
53. Porter AG, Janicke RU. Emerging roles of caspase-3 in apoptosis. Cell Death Differ 1999; 6:99–104.
54. Zheng TS, Schlosser SF, Dao T, Hingorani R, Crispe IN, Boyer JL, Flavell RA. Caspase-3 controls both cytoplasmic and nuclear events associated with Fas-mediated apoptosis in vivo. Proc Natl Acad Sci U S A 1998; 95:13618–13623.
55. Carbone MC, Pinto M, Antonelli F, Amicarelli F, Balata M, Belli M, Conti Devirgiliis L, Ioannucci L, Nisi S, Sapora O, Satta L, Simone G, et al. The Cosmic Silence experiment: on the putative adaptive role of environmental ionizing radiation. Radiat Environ Biophys 2009; 48:189–196.
56. Elmore E, Lao XY, Kapadia R, Giedzinski E, Limoli C, Redpath JL. Low doses of very low-dose-rate low-LET radiation suppress radiation-induced neoplastic transformation in vitro and induce an adaptive response. Radiat Res 2008; 169:311–318.
57. Ikushima T. Radio-adaptive response: characterization of a cytogenetic repair induced by low-level ionizing radiation in cultured Chinese hamster cells. Mutat Res 1989; 227:241–246.
58. Ikushima T, Aritomi H, Morisita J. Radioadaptive response: efficient repair of radiation-induced DNA damage in adapted cells. Mutat Res 1996; 358:193–198.
59. Satta L, Antonelli F, Belli M, Sapora O, Simone G, Sorrentino E, Tabocchini MA, Amicarelli F, Ara C, Ceru MP, Colafarina S, Conti Devirgiliis L, et al. Influence of a low background radiation environment on biochemical and biological responses in V79 cells. Radiat Environ Biophys 2002; 41:217–224.
60. Guo G, Yan-Sanders Y, Lyn-Cook BD, Wang T, Tamae D, Ogi J, Khaletskiy A, Li Z, Weydert C, Longmate JA, Huang TT, Spitz DR, et al. Manganese superoxide dismutase-mediated gene expression in radiation-induced adaptive responses. Mol Cell Biol 2003; 23:2362–2378.
61. Blaise R, Alapetite C, Masdehors P, Merle-Beral H, Roulin C, Delic J, Sabatier L. High levels of chromosome aberrations correlate with impaired in vitro radiation-induced apoptosis and DNA repair in human B-chronic lymphocytic leukaemia cells. Int J Radiat Biol 2002; 78:671–679.
62. Jeggo PA. The fidelity of repair of radiation damage. Radiat Prot Dosimetry 2002; 99:117–122.
63. Chang PY, Bjornstad KA, Rosen CJ, McNamara MP, Mancini R, Goldstein LE, Chylack LT, Blakely EA. Effects of iron ions, protons and X rays on human lens cell differentiation. Radiat Res 2005; 164:531–539.
64. Gougeon A. The biological aspects of risks of infertility due to age: the female side. Rev Epidemiol Sante Publique 2005; 53 Spec No 2: 2S37-2S45.
65. Richardson SJ, Nelson JF. Follicular depletion during the menopausal transition. Ann N Y Acad Sci 1990; 592:13–20.
66. te Velde ER, Scheffer GJ, Dorland M, Broekmans FJ, Fauser BC. Developmental and endocrine aspects of normal ovarian aging. Mol Cell Endocrinol 1998; 145:67–73.
67. Garg S, Boerma M, Wang J, Fu Q, Loose DS, Kumar KS, Hauer-Jensen M. Influence of sublethal total-body irradiation on immune cell populations in the intestinal mucosa. Radiat Res 2010; 173:469–478.
68. Gasser S, Raulet D. The DNA damage response, immunity and cancer. Semin Cancer Biol 2006; 16:344–347.
69. Gridley DS, Pecaut MJ, Nelson GA. Total-body irradiation with high-LET particles: acute and chronic effects on the immune system. Am J Physiol Regul Integr Comp Physiol 2002; 282:R677–R688.
70. Hoglund P. DNA damage and tumor surveillance R688: one trigger for two pathways. Sci STKE 2006. 2006: pe2.
71. Maverakis E, Miyamura Y, Bowen MP, Correa G, Ono Y, Goodarzi H. Light, including ultraviolet. J Autoimmun 2010; 34:J247–J257.
72. Zhang Q, Raoof M, Chen Y, Sumi Y, Sursal T, Junger W, Brohi K, Itagaki K, Hauser CJ. Circulating mitochondrial DAMPs cause inflammatory responses to injury. Nature 2010; 464:104–107.
73. Matikainen T, Perez GI, Zheng TS, Kluzak TR, Rueda BR, Flavell RA, Tilly JL. Caspase-3 gene knockout defines cell lineage specificity for programmed cell death signaling in the ovary. Endocrinology 2001; 142:2468–2480.
74. Bagshaw M. Cosmic radiation in commercial aviation. Travel Med Infect Dis 2008; 6:125–127.
75. Bottollier-Depois JF, Chau Q, Bouisset P, Kerlau G, Plawinski L, Lebaron-Jacobs L. Assessing exposure to cosmic radiation during long-haul flights. Radiat Res 2000; 153:526–532.
76. Bottollier-Depois JF, Chau Q, Bouisset P, Kerlau G, Plawinski L, Lebaron-Jacobs L. Assessing exposure to cosmic radiation on board aircraft. Adv Space Res 2003; 32:59–66.
77. Langner I, Blettner M, Gundestrup M, Storm H, Aspholm R, Auvinen A, Pukkala E, Hammer GP, Zeeb H, Hrafnkelsson J, Rafnsson V, Tulinius H, et al. Cosmic radiation and cancer mortality among airline pilots: results from a European cohort study (ESCAPE). Radiat Environ Biophys 2004; 42:247–256.